ECS Solid State Letters, **4** (5) R27-R30 (2015)
2162-8742/2015/4(5)/R27/4/$33.00 © The Electrochemical Society

Quantum Dot Light-Emitting Diodes for Uniform Eight-Segment Displays

Jia Zhao,[a] Yu Zhang,[a,b,z] Xiaoyu Zhang,[a] Yu Wang,[a] Siyao Yu,[a] Wenzhu Gao,[b] Hairong Chu,[c] Yiding Wang,[a] Jun Zhao,[d,e] and William W. Yu[a,d,e,z]

[a]*State Key Laboratory on Integrated Optoelectronics, College of Electronic Science and Engineering, Jilin University, Changchun 130012, People's Republic of China*
[b]*State Key Laboratory of Superhard Materials, College of Physics, Jilin University, Changchun 130012, People's Republic of China*
[c]*Changchun Institute of Optics, Fine Mechanics and Physics, Chinese Academy of Sciences, Changchun 130025, People's Republic of China*
[d]*Department of Chemistry and Physics, Louisiana State University, Shreveport, Louisiana 71115, USA*
[e]*College of Material Science and Engineering, Qingdao University of Science and Technology, Qingdao 266042, People's Republic of China*

Eight-segment LED displays were designed and fabricated using quantum dot light-emitting diodes. CdSe/CdS/ZnS core/shell quantum dot were employed as the emitting layer sandwiched by poly(N,N′-bis(4-butylphenyl)-N,N′-bis(phenyl)benzidine) (Poly-TPD) and an electron transport layer of ZnO nanoparticles. Each segment exhibited luminance, power efficiency and external quantum efficiency of 5380 cd/cm^2, 2.63 lm/W and 1.2%, respectively. The uniformity of the eight segments was analyzed based on the current-density and luminance versus driving voltage. The good uniformity indicates that the as-designed device is useful and promising for general electroluminescent display applications.
 [DOI: 10.1149/2.0041505ssl]

Manuscript submitted January 8, 2015; revised manuscript received March 2, 2015. Published March 11, 2015.

Semiconductor quantum dots (QDs) have great potentials as a unique optical material because of their inherent luminescent properties, including narrow spectral emission bandwidths, high photoluminescence quantum yield, good photostability, tunable emission wavelength that covers the entire visible region and extends to the infrared region.[1–6] Many potential applications exploiting the advantages of QDs have been suggested, such as optically or electrically pumped lasers,[7] sensors,[8,9] printable thin-film transistors (TFTs),[10] light-emitting diodes (LEDs),[11–13] and photovoltaics.[14,15]

In the past decade, quite a few research groups have demonstrated various LEDs using colloidal QDs as the active emitting layers.[16–20] There have been rapid advances in the specifications of luminance, efficiency, and lifetime of QD-LEDs,[16,17] which are even comparable to the well-developed organic light-emitting devices (OLEDs). The QD displays have a more accurate color representation than OLED displays,[18,21] so QDs are potential to simultaneously improve the material stability, lifetime, efficiency, and color purity of OLEDs, while allowing solution-processing techniques in large-area manufacturing.[22] Frontier Research Lab made a display image of a 4-inch cross-linked QD-LED using an a-Si TFT backplane with a 320×240 pixel array for the active matrix drive.[17] Samsung Electronics Advanced Institute of Technology demonstrated full color QD display using a method of transfer printing which had a good quality of brightness and efficiency.[20,23]

In this work, we fabricated bright, efficient eight-segment QD-LED displays using CdSe/CdS/ZnS QDs with a simple drive circuit. The QD-LED exhibited a high luminance and a good quality of uniformity.

Experimental

Chemicals.— Cadmium oxide (CdO, 99.998%), selenium (Se, 99.999%), 1-octadecene (ODE, 90%), oleic acid (OA, 90%), sodium hydroxide (NaOH, 98%), zinc acetate ($Zn(CH_3COO)_2$, 99.98%) and octadecylamine (ODA, 98%) were purchased from Alfa Aesar. Trioctylphosphine oxide (TOPO, 90%), hexadecylamine (HDA, 90%) and trioctylphosphorus (TOP, 97%) were purchased from Sigma-Aldrich. Zinc oxide (ZnO, 99.99%) and sulfur (S, 99.99%) were purchased from Aladdin. All organic solvents were purchased from Sigma-Aldrich. The chemicals were used directly without further treatment.

Synthesis of CdSe Core QDs.— In a typical synthesis,[2,3] the mixture of 0.2 mmol of CdO, 0.8 mmol of OA and 8 ml ODE in a 25 ml three-neck flask was heated to 220°C under N_2 to obtain a colorless solution. After cooled to room temperature, 1.5 g of HDA and 1.5 g of TOPO were added into the flask, and reheated to 270°C. Then, a selenium solution made by dissolving 2 mmol of Se in 2 ml of TOP was swiftly injected into the flask. The growth temperature was immediately reduced to 250°C. The injection temperature and reaction time were tuned to obtain the CdSe QDs with different emission peaks. The reaction mixture was cooled to room temperature, and an extraction procedure was used to purify the QDs from side products and unreacted precursors.[24–26]

Injection solutions.— The cadmium precursor solution (0.04 mol/L) was prepared by dissolving CdO (0.0448 g) with OA (0.5935 g) in ODE (8 ml) at 250°C. The sulfur precursor solution (0.04 mol/L) was prepared by dissolving sulfur powder (0.0257 g) in ODE (20 ml) at 150°C. The zinc precursor solution (0.04 mol/L) was prepared by dissolving ZnO (0.0228 g) with OA (0.3162 g) in ODE (6.86 ml) at 250°C. After clear solutions were obtained under N_2 flow, the Cd, sulfur, zinc injection solution were allowed to cool to 60°C, 25°C, 100°C when used for injection.

Synthesis of CdSe/CdS/ZnS core/shell QDs.— For shell growth, CdSe QDs dispersed in 2 ml of hexanes were loaded into a 100 ml three-neck flask and mixed with 4.53 g ODA and 19.41 g ODE. The reaction mixture was heated to 200°C under N_2 flow. Then, the predetermined volumes of the cadmium, zinc and sulfur solutions were alternatively injected into the three-neck flask drop by drop with syringes using standard air-free procedures. The reaction time for each anion and cation layer was 10 min. The shell growth was stopped by the injection of room-temperature toluene, then the core/shell QDs were purified and redispersed in toluene for characterization and device fabrication.[2,3,27]

Synthesis of ZnO nanocrystals.— A mixture of 0.44 g zinc acetate and 30 ml ethanol was loaded into a three-neck flask and heated to 75°C until a clear solution was obtained. After the solution was cooled down to room temperature, 10 ml of NaOH/ethanol solution (0.5 mol/L) was injected into the flask. The solution was stirred for 12 h, and the products were collected by precipitating with hexanes and redispersed in ethanol for device fabrication.[28]

[z]E-mail: yuzhang@jlu.edu.cn; wyu6000@gmail.com

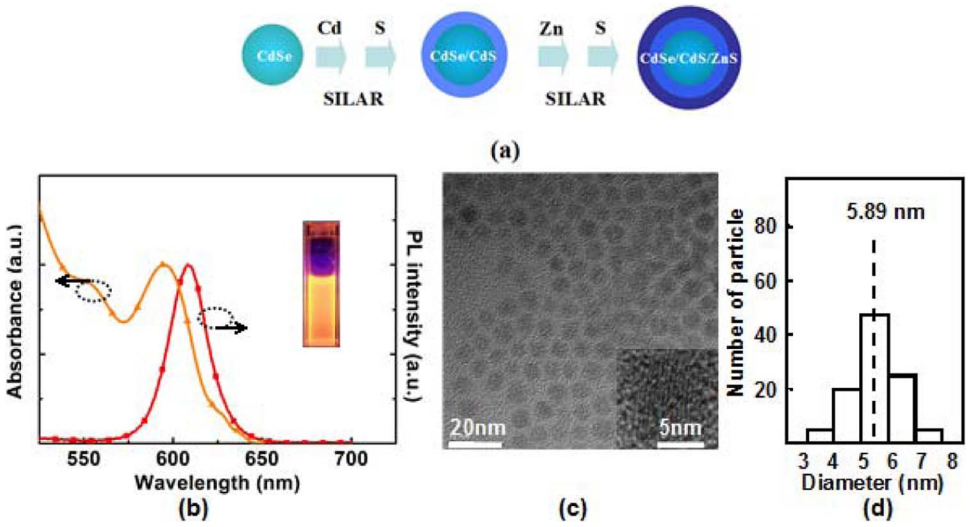

Figure 1. Structure of CdSe/CdS/ZnS QD (a), Abs and PL spectra with a red emitting picture (b), TEM images (c), and size distribution (d) of CdSe/CdS/ZnS QDs.

Eight-segment QD-LED display fabrication.— The ITO on the glass substrate was etched into the designed pattern. Then, the substrate was cleaned with deionized water, acetone and isopropanol, consecutively, for 15 min. After that the patterned ITO glass was treated with UV-ozone. Poly (ethylenedioxythiophene): polystyrene sulfonate (PEDOT:PSS) were deposited on the ITO by spin-coating and baked at 150°C for 15 min. The coated substrate was then transferred to a N_2-filled glove box for spin-coating of Poly-TPD, CdSe/CdS/ZnS QDs and ZnO nanoparticle layers. The Poly-TPD hole-transport layer was spin-coated using 1.5 wt% in chlorobenzene (2,000 r.p.m. for 30 s), followed by baking at 110°C for 30 min. This was followed by spin-coating of CdSe/CdS/ZnS QDs (10 mg/ml in toluene, 2,000 r.p.m) and ZnO nanoparticles (30 mg/ml in ethanol, 4,000 r.p.m) layers followed by baking at 80°C for 30 min.[16] Al cathode was patterned by an in-situ shadow mask to form active device areas of 1.5 mm × 7 mm. The size of the whole device was 1.2 cm × 2 cm.

Results and Discussion

CdSe QDs were prepared in noncoordinating solvent[29,30] and successively coated with CdS and ZnS shells by using successive ion layer adsorption and reaction.[2,3,27] Two monolayers of CdS were covered on the surface of CdSe core with a thickness of 0.35 nm each and two monolayers of ZnS were grown on the surface of CdSe/CdS with a thickness of 0.32 nm each as shown in Figure 1a. Figure 1b shows the Abs and PL spectra of the as-prepared CdSe/CdS/ZnS QDs, which exhibited a quantum yield of 50% determined by a fluorescence spectrometer (FLS920P, Edinburgh Instruments) with an integrating sphere. The Abs and PL peaks of CdSe/CdS/ZnS QDs were 598 nm and 608 nm, respectively, while FWHM of PL peak was 28 nm. An average particle size of 5.89 was determined from TEM images and the size distribution shown in Figure 1c. Lattice fringes could be clearly observed in the high-resolution TEM image shown in the inset, which suggested good crystallinity of the CdSe/CdS/ZnS QDs.

The structure of QD-LEDs employed in this work is schematically shown in Figure 2a. According to the schematic energy level diagram shown in Figure 2b, with an electron affinity of −4.3 eV and an ionization potential of −7.6 eV, the ZnO nanoparticle layer not only provides efficient electron injection from the Al cathode into CdSe/CdS/ZnS QDs, but also helps to confine holes within the QD layer due to the valence band offset at the QD/ZnO nanoparticle interface, leading to an improved charge recombination efficiency. ZnO nanoparticle film was used in this structure as the electron transport layer because the conduction band of ZnO is aligned with the Fermi level of Al leading to low energy barriers for electron injection from the cathode into the EML (emitting layer) and its high electron mobility. Electrons and holes can be efficiently injected into the QD EML at low driving voltages. Because of the large energy offset at this type II heterojunction, holes and electrons are likely to accumulate at the interface between Poly-TPD and the QD EML. The Auger assisted hole injection process can take place owing to the accumulation of opposite charges at the interface.[16]

We designed and etched the ITO on the glass into four strips. The cathode template was hollowed out five strips and Al cathode was deposited by vacuum thermal evaporation method crossing with ITO. Figure 3a shows current density and luminance curves as a function of applied voltage for one segment of the eight-segment device. The turn on voltage of the device was about 3.5 V, while the maximum luminance reached 5380 cd/m^2. The device has low turn-on and operating voltages because of the structure we used. The low driving voltages for the QD-LEDs are expected to lead to higher power efficiency and better device stability. The highest power efficiency (PE) of 2.63 lm/W and external quantum efficiency (EQE) of 1.2% which are plotted in Figure 3b were achieved while the current density was about 0.1 mA/cm^2. The EL spectra at different voltages are

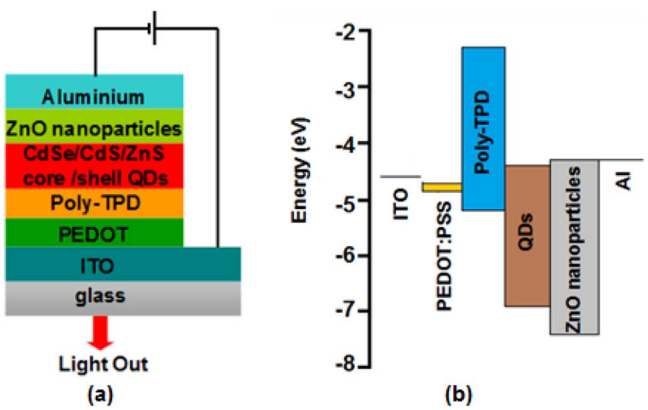

Figure 2. (a) The structure of the QD-LED; (b) Energy level diagram for the various layers of device.

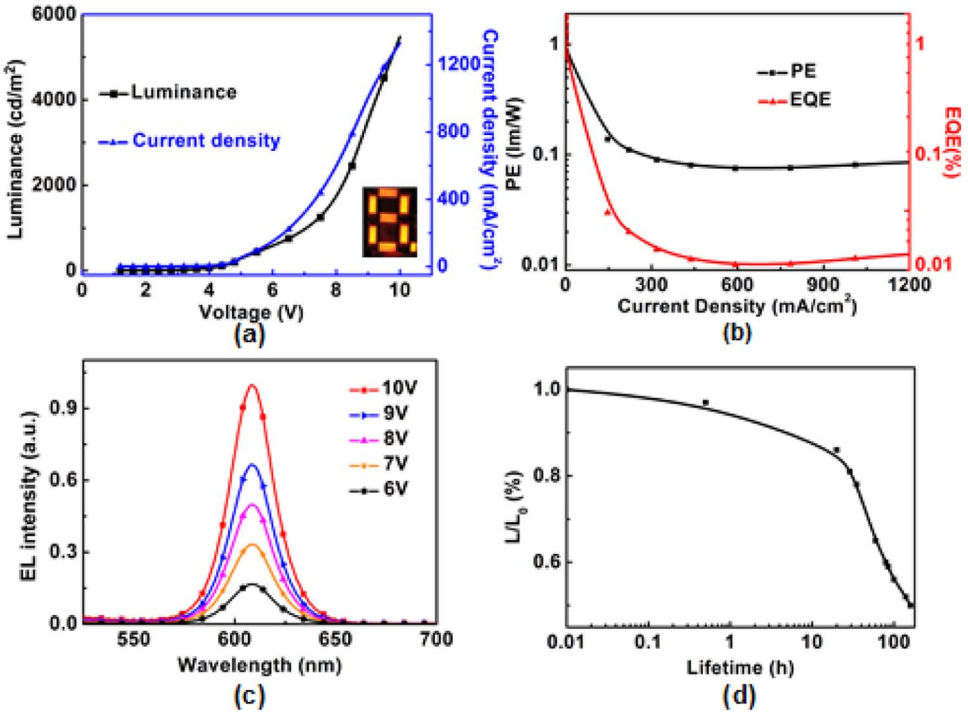

Figure 3. (a) Current density and luminance versus driving voltage of one segment of the eight-segment device. The inset shows the picture of the eight segments. (b) PE (lm/W) and EQE (%) versus current density (mA/cm^2). (c) EL spectra at different voltages of one segment of the eight-segment device. (d) The degradation of the brightness for one segment of the device. L_0 was the initial luminance at 100 cd/m^2.

shown in Figure 3c. The emission of the QD-LED peaked at 613 nm which shifted to red for 5 nm compared with the PL spectra. The lifetime of one segment was tested to be 160 h under N_2 at an initial luminance of 100 cd/cm^2 (Figure 3d). The possible reasons for the degradation of device were the increase of area and number of nonemissive regions or dark spot defects with the extended working time.[31]

The uniformity of the eight-segment device was analyzed by comparing the performance of eight segments of as-fabricated device as shown in Figure 4. The luminance of the eight segments from 'a' to 'h' were nearly the same at the same voltages as shown in Figure 4a. The similar behavior of carrier injection was also observed at the driving voltages from 0 to 10 V which indicated the uniform film deposited on the substrate in the whole device area. Figure 4c shows the luminance of every segment was nearly 4000 cd/m^2 and the current density of every segment was nearly 800 mA/cm^2 at 8.8 V. Thus the as-fabricated QD-based eight-segment device exhibited a good quality of uniformity.

Conclusions

We have demonstrated bright and efficient QD-based eight-segment displays using CdSe/CdS/ZnS QDs. The devices showed a maximum luminance of 5380 cd/cm^2, PE of 2.63 lm/W, and EQE of 1.2%. As we all know, eight-segment displays are widely used in many electronic instruments. This work built a model for broad applications of QD-LEDs, which indicates the prosperous future of QD-based display products.

Acknowledgment

This work was financially supported by the National Natural Science Foundation of China (61106039, 51272084, 61306078, 61225018, 61475062), the National Postdoctoral Foundation (2011049015), the Jilin Province Key Fund (20140204079GX), the State Key Laboratory on Integrated Optoelectronics (IOSKL2012ZZ12), the Taishan Scholarship, the Shandong Natural Science Foundation (ZR2012FZ007), and NSF (1338346).

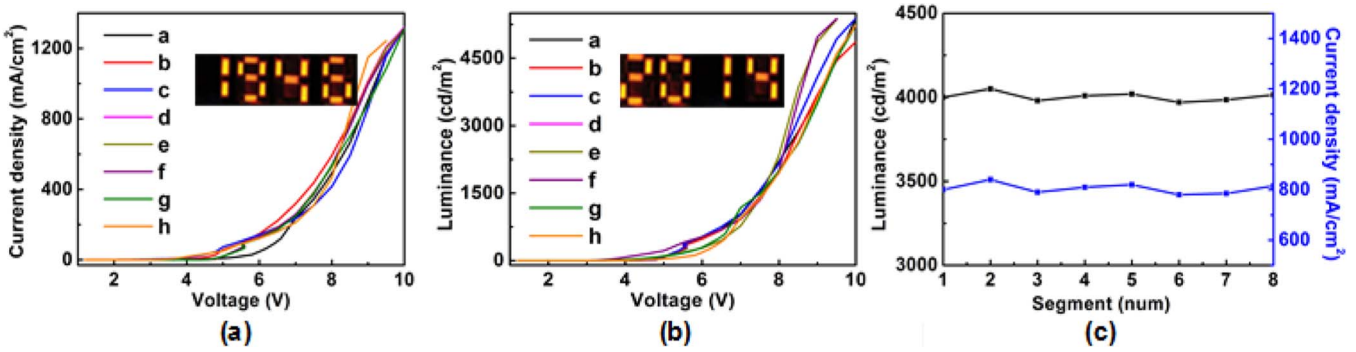

Figure 4. (a) Current–density versus driving voltage of eight-segment QD-LED display. (b) Luminance versus driving voltage of eight-segment QD-LED display. The letters of a-h stand for the eight segments of the display, respectively. (c) Trend of current density and luminance for the eight segments at the same voltage.

References

1. W. W. Yu, L Qu, W Guo, and X Peng, *Chemistry of Materials*, **15**(14), 2854 (2003).
2. J. J. Li, Y. A. Wang, W. Guo, J. C. Keay, T. D. Mishima, M. B. Johnson, and X. Peng, *Journal of the American Chemical Society*, **125**(41), 12567 (2003).
3. J.-J. Hao, J. Zhou, and C.-Y. Zhang, *Chemical Communications*, **49**(56), 6346 (2013).
4. B. Xing, W. W. Li, H. J. Dou, P. F. Zhang, and K. Sun, *Journal of Physical Chemistry C*, **112**(37), 14318 (2008).
5. W. K. Bae, K. Char, H. Hur, and S. Lee, *Chemistry of Materials*, **20**(2), 531 (2008).
6. O. Chen, J. Zhao, V. P. Chauhan, J. Cui, C. Wong, D. K. Harris, H. Wei, H.-S. Han, D. Fukumura, R. K. Jain, and M. G. Bawendi, *Nature Materials*, **12**(5), 445 (2013).
7. V. I. Klimov, A. A. Mikhailovsky, S. Xu, A. Malko, J. A. Hollingsworth, C. A. Leatherdale, H. J. Eisler, and M. G. Bawendi, *Science*, **290**(5490), 314 (2000).
8. P. Gu, Y. Zhang, Y. Feng, T. Zhang, R. Chu, T. Cui, Y. Wang, J. Zhao, and W. W. Yu, *Nanoscale*, **5**(21), 10481 (2013).
9. L. Yan, Y. Zhang, T. Zhang, Y. Feng, K. Zhu, D. Wang, T. Cui, J. Yin, Y. Wang, J. Zhao, and W. W. Yu, *Analytical Chemistry*, **86**, 11312 (2014).
10. Y.-C. Chen, C.-Y. Huang, H.-C. Yu, and Y.-K. Su, *Journal of Applied Physics*, **112**(3), 34518 (2012).
11. X. Y. Yang, E. Mutlugun, C. Dang, K. Dev, Y. Gao, S. T. Tan, X. W. Sun, and H. V. Demir, *American Chemical Society Nano*, **8**, 8224 (2014).
12. Y. Zhang, C. Xie, H. Su, J. Liu, S. Pickering, Y. Wang, W. W. Yu, J. Wang, Y. Wang, J. Hahm, N. Dellas, S. E. Mohney, and J. Xu, *Nano Letters*, **11**(2), 329 (2011).
13. C. Sun, Y. Zhang, Y. Wang, W. Liu, S. Kalytchuk, S. V. Kershaw, T. Zhang, X. Zhang, J. Zhao, W. W. Yu, and A. L. Rogach, *Applied Physics Letters*, **104**(26), 201106 (2014).
14. N. Tessler, V. Medvedev, M. Kazes, S. Kan, and U. Banin, *Science*, **295**(5559), 1506 (2002).
15. X. Li, H. Shen, W. Wang, J. Li, and H. Lin, *Chinese Science Bulletin*, **59**(25), 3209 (2014).
16. L. Qian, Y. Zheng, J. Xue, and P. H. Holloway, *Nature Photonics*, **5**(9), 543 (2011).
17. K. S. Cho, E. K. Lee, W. J. Joo, E. Jang, T. H. Kim, S. J. Lee, S. J. Kwon, J. Y. Han, B. K. Kim, B. L. Choi, and J. M. Kim, *Nature Photonics*, **3**(6), 341 (2009).
18. P. O. Anikeeva, J. E. Halpert, M. G. Bawendi, and V. Bulovic, *Nano Letters*, **9**(7), 2532 (2009).
19. Q. Sun, Y. A. Wang, L. Li, D. Wang, T. Zhu, J. Xu, C. Yang, and Y. Li, *Nature Photonics*, **1**(12), 717 (2007).
20. T. H. Kim, K. S. Cho, E. K. Lee, S. J. Lee, J. Chae, J. W. Kim, D. H. Kim, J. Y. Kwon, G. Amaratunga, S. Y. Lee, B. L. Choi, Y. Kuk, J. M. Kim, and K. Kim, *Nature Photonics*, **5**(3), 176 (2011).
21. F. Zhang, J. Xue, Z. Yu, W. Zhou, and G. Hui, *Chinese Journal of Liquid Crystals and Displays*, **2**(24) 163 (2012).
22. G. Moeller and S. Coe-Sullivan, *Information Display*, **22**(2), 32 (2006).
23. T. H. Kim, S. Jun, K. S. Cho, B. L. Choi, and E. Jang, *MRS Bulletin*, **38**(9), 712 (2013).
24. Y. Zhang, Q. Dai, X. Li, B. Zou, Y. Wang, and W. W. Yu, *Journal of Nanoparticle Research*, **13**(9), 3721 (2011).
25. W. Liu, Y. Zhang, W. Zhai, Y. Wang, T. Zhang, P. Gu, H. Chu, H. Zhang, T. Cui, Y. Wang, J. Zhao, and W. W. Yu, *The Journal of Physical Chemistry C*, **117**(38), 19288 (2013).
26. J. Zhang and W. W. Yu, *Applied Physics Letters*, **89**(12), 123108 (2006).
27. Y. Zhang, Q. Dai, X. Li, J. Liang, V. L. Colvin, Y. Wang, and W. W. Yu, *Langmuir*, **27**(15), 9583 (2011).
28. X. Zhang, Y. Zhang, Y. Wang, S. Kalytchuk, S. V. Kershaw, Y. Wang, P. Wang, T. Zhang, Y. Zhao, H. Zhang, T. Cui, Y. Wang, J. Zhao, W. W. Yu, and A. L. Rogach, *ACS Nano*, **7**(12), 11234 (2013).
29. W. W. Yu, Y. A. Wang, and X. Peng, *Chemistry of Materials*, **15**(22), 4300 (2003).
30. Y. Zhang, Q. Dai, X. Li, Q. Cui, Z. Gu, B. Zou, Y. Wang, and W. W. Yu, *Nanoscale Research Letters*, **5**(8), 1279 (2010).
31. P. E. Burrows, V. Bulovic, S. R. Forrest, L. S. Sapochak, D. M. McCarty, and M. E. Thompson, *Applied Physics Letters*, **65** (23), 5 (1994).